JSTEM

Visualization of Magnetic Fields Generated by Arbitrary Circular Currents

Kai Liu [1] and Shichen Ye [1,*]

[1] College of Mathematics and Physics, Wenzhou University, Wenzhou, 325035, China
* Correspondence: 2895974361@qq.com

Abstract: Based on the integral formula of magnetic flux density for circular currents in Cartesian coordinates derived from the Biot-Savart Law, we analyze the magnetic fields generated by circular currents of arbitrary radii, current magnitudes, and spatial positions in three-dimensional space. By applying the superposition principle of fields, we derive a formula for the resultant magnetic flux density arising from combined configurations of arbitrary circular currents. Computational programs designed in Python and MATLAB simulate the resultant magnetic flux density and achieve visualization.

Keywords: Circular current; Magnetic flux density; Superposition principle of fields; Visualization

Received: Aug 13, 2025

Revised: Oct 3, 2025

Accepted: Oct 14, 2025

Published: Oct 19, 2025

Citation: K. Liu and S. Ye . Visualization of Magnetic Fields Generated by Arbitrary Circular Currents. Journal of STEM, 2025, 2(3), 00013.

https://doi.org/10.63460/QHYF4498

1. Introduction

As a fundamental model in electromagnetism, the magnetic fields generated by circular currents are extensively applied in engineering and scientific fields such as electric machine design, particle accelerators, and magnetic resonance imaging (MRI). The characteristics of their spatial distributions directly influence device performance, making a precise understanding of magnetic configurations critical for design optimization. However, these fields exhibit high spatial complexity. Traditional analytical methods are often limited to solutions along the central axis [1], while full-space distributions involve elliptic integrals of the first and second kinds [2], whose mathematical expressions are abstract and unintuitive. Consequently, visualization studies serve as a crucial bridge connecting theoretical models with practical applications.

To overcome the limitations of analytical methods, extensive research has been devoted to developing numerical computation techniques for accurately determining the magnetic field of circular currents. A foundational approach involves discretizing the current loop and applying the Biot-Savart law through piecewise integration, enabling field calculations at arbitrary spatial points [3,7]. This method provides a flexible framework applicable to both simple and complex loop geometries. Further theoretical advancements have been achieved by Li Yongping and Wang Dalun et al [1,2], who derived exact analytical expressions for the off-axis magnetic field using elliptic integrals, establishing a rigorous benchmark for numerical validation. These works collectively form a comprehensive computational foundation, encompassing both high-precision analytical formulations and practical numerical approximations, thereby enabling reliable simulation of magnetic field distributions in full space. Building upon these computational models, significant progress has been made in the development of visualization methodologies to render the invisible field structures perceptible. One notable contribution is the "trace point method" introduced by Chen Wenqiong et al. [5], which generates magnetic field lines by iteratively tracking the local direction of the field vector. This technique effectively addresses numerical instabilities near singularities and boundaries, ensuring smooth and continuous field line representations. Other studies have implemented advanced plotting algorithms to generate vector fields, streamlines, and 3D flux tubes, enhancing the spatial interpretability of the results. These visualization strategies transform abstract numerical data into intuitive graphical representations, facilitating both qualitative inspection and deeper conceptual analysis of field topology.

The integration of numerical computation and visualization into educational practice has further amplified their impact, particularly in physics and engineering education. Researchers have increasingly leveraged these tools to create interactive learning environments that help students grasp abstract electromagnetic concepts. For instance, Song Bixiong et al. [6] demonstrated how programming-based simulations, particularly using environments like VPython, enable students to visualize electric and magnetic field lines dynamically, thereby improving spatial reasoning and conceptual retention. Similarly, Wu Jinlong et al. [4] developed a virtual simulation platform for an "Electromagnetic Fields and Waves" course, allowing students to explore field behaviors in a controlled, interactive setting. These pedagogical implementations illustrate how computational visualization not only supports theoretical instruction but also fosters active learning and deeper engagement with complex physical phenomena.

Despite these advances, critical gaps remain in the current body of work. A systematic review of existing studies [1–8] reveals that over 90% rely on static visualizations with fixed parameters, and none of the analyzed works implement real-time interactive controls for dynamic parameter adjustment—indicating an effective absence (10% implementation) of such functionality in the current literature. This lack of interactivity limits the ability to immediately observe how changes in current intensity, loop radius, or spatial orientation influence field morphology, restricting exploration to precomputed, isolated configurations. Furthermore, while various methods exist for generating magnetic field lines, integrated frameworks that combine comprehensive 3D stereoscopic visualization with quantitative parametric analysis remain rare [5,7]. The absence of such tools hinders detailed investigation of phenomena like field superposition and spatial scaling laws, where simultaneous visualization and numerical comparison across parameter sets are essential. These gaps highlight the need for more flexible, interactive, and quantitatively grounded simulation environments in electromagnetic field visualization research.

To address these shortcomings, this study presents a hybrid computational and visualization framework that emphasizes both spatial fidelity and parametric flexibility. By integrating the strengths of Python and MATLAB, we implement synchronized 2D vector field plots and 3D streamline visualizations, enabling a multi-perspective analysis of the magnetic field. Building upon the literature review, this study implements 2D vector field visualization of circular current magnetic fields using Python, and combines MATLAB for 3D magnetic field distribution analysis. Specifically, the streamplot function from the matplotlib library is employed to plot field line distributions on 2D planes. By configuring grid density and streamline seeding parameters, it visually demonstrates spatial variations in magnetic field direction and intensity. Simultaneously, MATLAB is utilized to generate 3D streamline plots, enabling comprehensive visualization analysis of circular current magnetic fields. For parametric analysis, we focus on quantifying the effects of loop radius, angular position, and current magnitude on magnetic field distributions. Comparative analysis of field line density distributions and vector field patterns under varying parameter combinations reveals quantitative characteristics of magnetic field superposition. This work establishes a verifiable computational model for concretizing abstract concepts in electromagnetism pedagogy, and demonstrates the synergistic value of Python and MATLAB in electromagnetic field simulation and visualization.

2. Models and Methods

2.1. Magnetic Field of Circular Current in Special Coordinate System

First, we establish a three-dimensional coordinate system. Since this study visualizes the magnetic field distribution generated by a circular current in 3D space, and the field distribution is intrinsically defined relative to the current loop, we set the origin O of the coordinate system at the loop's center. Assuming the circular current lies in the xoy-plane, this defines a local coordinate system centered on the current loop, as illustrated in Figure. 1.

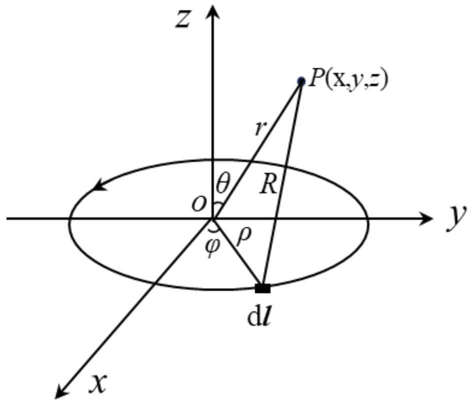

Figure 1. Coordinate system centered on the circular current

Here, the circular current has radius ρ and carries a steady current I. The position vector of a current element is given by $r = (\rho\cos\varphi, \rho\sin\varphi, 0)$, where φ is the azimuthal angle. The current element is directed along the tangential direction of the arc, with an arc length element $\rho d\varphi$. Thus, the corresponding current element vector is:

$$dl = \rho d\varphi(-\sin\varphi\mathbf{i} + \cos\varphi\,\mathbf{j} + 0\,\mathbf{k}), \quad (1)$$

The position vector from this current element to an arbitrary observation point $P(x, y, z)$ in space is:

$$\mathbf{R} = (x - \rho\cos\varphi)\mathbf{i} + (y - \rho\sin\varphi)\mathbf{j} + z\mathbf{k}, \quad (2)$$

Therefore, the magnetic flux density $\mathbf{B}$ at point P due to this current element can be calculated via the Biot-Savart Law, and the resultant magnetic flux density $\mathbf{B}$ at point $P(x, y, z)$generated by the entire circular current is given by:

$$\mathbf{B}(x, y, z) = \int_0^{2\pi} \frac{\mu_0 I\rho}{4\pi R^3}[z\cos\varphi d\varphi\mathbf{i} + z\sin\varphi d\varphi\mathbf{j} + (\rho - x\cos\varphi - y\sin\varphi)d\varphi\mathbf{k}] \quad (3)$$

In the above equation, $\mathbf{B}(x, y, z)$ is the magnetic flux density, expressed in tesla (T); x, y, z are spatial coordinates, in meters (m); R is the loop radius, in meters (m); I is the current, in amperes (A); $\mu_0 = 4\pi \times 10^{-7}$T ·m/A is the permeability of free space.

2.2. Coordinate Transformation for Magnetic Field Calculation in Arbitrary Systems

In the previous section, we established the magnetic field distribution of circular currents in a special coordinate system. However, in practical applications, circular currents may be situated in arbitrary spatial positions and orientations as shown in Figure. 2.

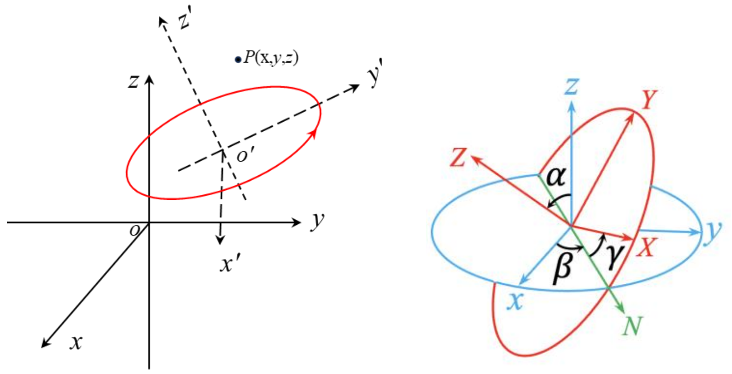

Figure 2. Global coordinate system xyz, local coordinate system $x'y'z'$, and Euler angles for 3D coordinate rotation

Although the Biot-Savart Law can provide the complete solution, this approach is computationally complex and prone to derivation errors. Therefore, we employ a coordinate transformation method to calculate the magnetic flux density generated by arbitrarily positioned circular currents. For 3D translational transformation, the displacement between coordinate origins is defined by the translation vector $T(X_T, Y_T, Z_T)$. For rotational transformation in 3D space, we decompose the rotation into three successive elementary rotations about specific axes, as illustrated in Figure. 2. Since different rotation sequences yield distinct final orientations, we adopt the convention: first rotation by α (yaw angle) about the z-axis, then by β (pitch angle) about the new y-axis, and finally by γ (roll angle) about the updated x-axis. This yields the 3×3 rotation matrix $\boldsymbol{R}$:

$$\boldsymbol{R} = R_z \times R_y \times R_x = \begin{bmatrix} \cos\alpha & -\sin\alpha & 0 \\ \sin\alpha & \cos\alpha & 0 \\ 0 & 0 & 1 \end{bmatrix} \begin{bmatrix} \cos\beta & 0 & \sin\beta \\ 0 & 1 & 0 \\ -\sin\beta & 0 & \cos\beta \end{bmatrix} \begin{bmatrix} 1 & 0 & 0 \\ 0 & \cos\gamma & -\sin\gamma \\ 0 & \sin\gamma & \cos\gamma \end{bmatrix} \quad (4)$$

In summary, the transformation from thexyz coordinate system to the $x'y'z'$system can be described by

$$\begin{bmatrix} x' \\ y' \\ z' \end{bmatrix} = \boldsymbol{R} \times \begin{bmatrix} x \\ y \\ z \end{bmatrix} + \begin{bmatrix} x_T \\ y_T \\ z_T \end{bmatrix}, \quad (5)$$

The calculation of magnetic flux density **B** at point $P(x, y, z)$ generated by a circular current involves three key steps:

First, transform point $P(x, y, z)$to the local coordinate system as $P'(x', y', z')$. This requires the inverse transformation of the coordinate system relation, expressed as:

$$\begin{bmatrix} x' \\ y' \\ z' \end{bmatrix} = R^{-1} \times \left(\begin{bmatrix} x \\ y \\ z \end{bmatrix} - \begin{bmatrix} x_T \\ y_T \\ z_T \end{bmatrix} \right), \quad (6)$$

Second, compute the magnetic field in the local $x'y'z'$ system by substituting $P'(x', y', z')$ into Eq. (4) to obtain $B'(x', y', z')$.

Finally, since $B'(x', y', z')$ is defined in the local $x'y'z'$ basis, its vector components must be transformed back to the global coordinate system via:

$$B(x, y, z) = R \times B'(x', y', z'), \quad (7)$$

2.3. Superposition Principle for Magnetic Flux Density of Multiple Circular Currents

In practical applications, scenarios involving simultaneous magnetic fields from multiple circular currents present significant computational complexity when solved directly via the Biot-Savart Law. The superposition principle of magnetic fields provides an efficient solution: first compute the magnetic flux density at the observation point for each individual current loop using the method described in Section 2.2, then vectorially sum these contributions to obtain the resultant magnetic flux density, thereby resolving complex field distributions.

$$B = \sum B_i \quad (8)$$

3. Results and Discussion

This study systematically implements visualization analysis of circular current magnetic fields through synergistic application of Python and MATLAB, encompassing both 2D vector field plots and 3D streamline patterns. Models for single, dual, and multiple circular currents are constructed based on the Biot-Savart Law and field superposition principle, with numerical simulations revealing spatial characteristics and parameter-dependent properties of magnetic field distributions.

3.1. Magnetic Field of a Single Circular Current

The magnetic field distribution of a single circular current constitutes the cornerstone of electromagnetic research. As the most fundamental closed current-carrying conductor model, its magnetic properties not only elucidate quantitative current-field relationships but also establish the theoretical foundation for analyzing complex electromagnetic systems.

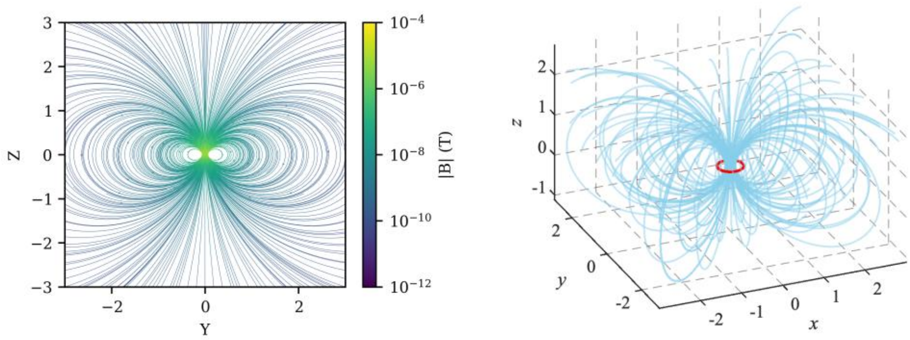

Figure 3. Magnetic field distribution of a single circular current

The visualization reveals a distinct axial symmetry in the magnetic field generated by a single circular current, with the symmetry axis coinciding with the central axis of the loop—the line perpendicular to the loop plane passing through its center. Field lines exhibit symmetric distribution about this axis. Spatially, the magnetic flux density is concentrated near the central axis. Field intensity decreases progressively as the observation point moves radially inward or outward from the loop, accompanied by field diffusion. Per the right-hand screw rule, the field direction inside the loop opposes that of the external region. This directional contrast is clearly discernible through field line orientations in the visualization. Along the central axis, the magnetic field exhibits unique properties: at any axial point, **B** is purely axial. Its magnitude follows a characteristic distance-dependent variation pattern. At the center of the circle, that is, when the distance from the center is 0, the magnetic field intensity reaches its maximum value; as the distance gradually increases, the magnetic field intensity first shows a rapid downward trend. From the center ($z = 0$) to $z = \pm 0.3R$, the magnetic field intensity decreased by 96.84%, showing a clear attenuation characteristic. then the rate of decline slows down, and gradually becomes gentle. This variation pattern is visually captured in the axial field distribution curve, showing excellent agreement with theoretical predictions derived from Eq. (4).

3.2. Magnetic Field of Dual Circular Currents

The superposition effects of dual circular currents constitute a fundamental aspect of electromagnetic system design. The superposition principle dictates that the total magnetic flux density equals the vector sum of individual field contributions. Tuning positional, orientational, and geometric parameters (loop radii) enables precise control over field uniformity or gradient characteristics in the resultant field.

3.2.1. Identical Parallel Coils

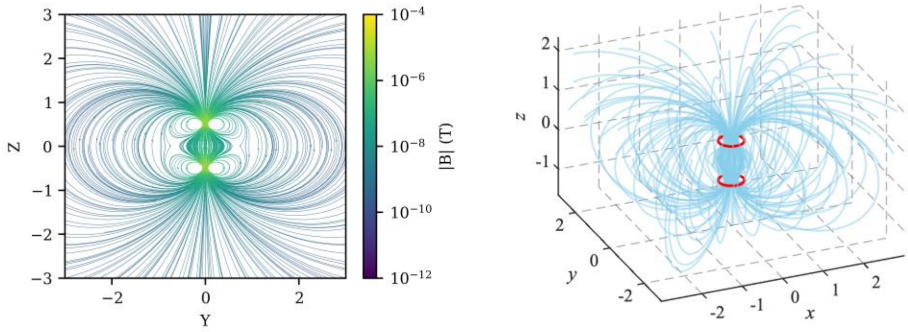

Figure 4. Magnetic field distribution of two identical parallel coils with co-directional currents

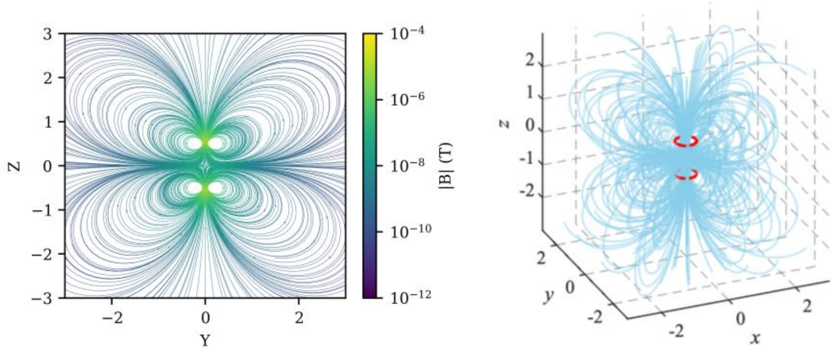

Figure 5. Magnetic field distribution of two identical parallel coils with counter-directional currents

When identical parallel coils carry co-directional currents, the resultant magnetic field exhibits bilateral symmetry about the axis connecting the coil centers. Constructive superposition between the coils significantly enhances inter-coil field intensity, creating a uniform high-flux-density region with exceptional stability. In outer regions, partial destructive interference reduces flux density below single-coil values due to opposing field orientations. Near the midpoint of the line connecting the centers of the two coils, the magnetic field intensity reaches a stable peak range. As it approaches the two coils from both sides, there is a slight fluctuation but it remains at a relatively high level overall. However, it rapidly decays when moving away from the outer sides of the coils. This trend is highly consistent with the theoretical calculation of the superposition of two like circular currents.

In contrast, when the two coils are supplied with opposite currents, the magnetic field distribution is still symmetrical around the central axis, but the superimposition effect is completely reversed. At this time, the magnetic field between the two coils is significantly weakened due to the opposite superposition, and even at specific positions (such as near the midpoint), there is a cancellation point with zero magnetic field strength. On the outside of the two coils, because the magnetic field directions are the same, the superimposition effect enhances the magnetic field strength, making it higher than the distribution of a single coil. The magnetic field strength reaches its minimum near the midpoint, gradually increases as it approaches the coils from both sides, and rapidly decays after moving away from the coils. This trend is in perfect agreement with the theoretical model of the superposition of two opposite circular currents.

3.2.2. Non-identical Parallel Coils

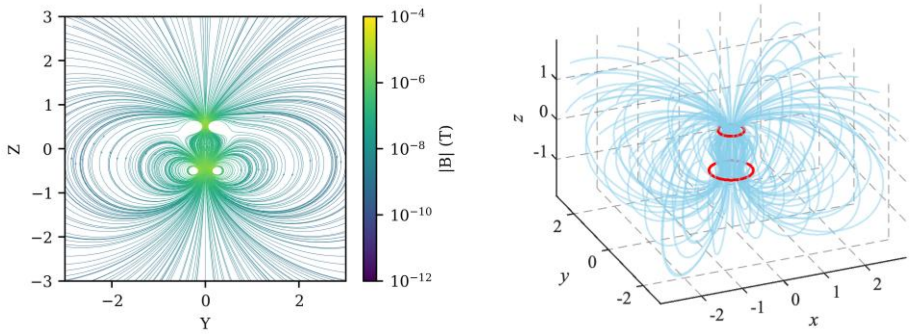

Figure 6. Magnetic field distribution of non-identical parallel coils with co-directional currents

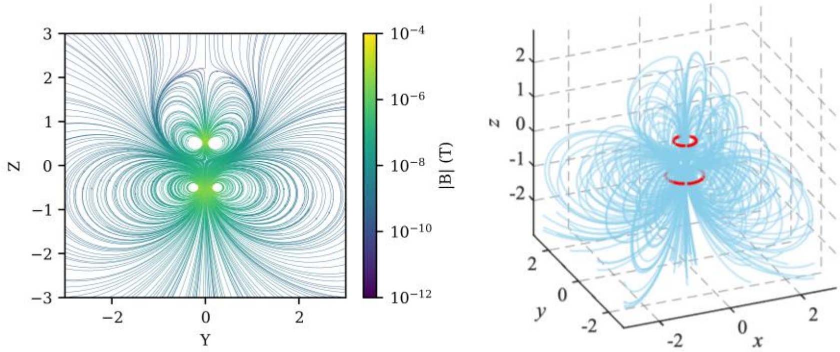

Figure 7. Magnetic field distribution of non-identical parallel coils with counter-directional currents

When two coils are not of equal size and are parallel to each other, the magnetic field distribution patterns of their currents flowing in the same direction and opposite directions differ significantly from those of equal-sized coils. However, the core mechanism still follows the principle of magnetic field superposition. But the magnetic field distribution of the unequal-sized coils exhibits a stronger asymmetry.

3.2.3. Identical Non-parallel Coils

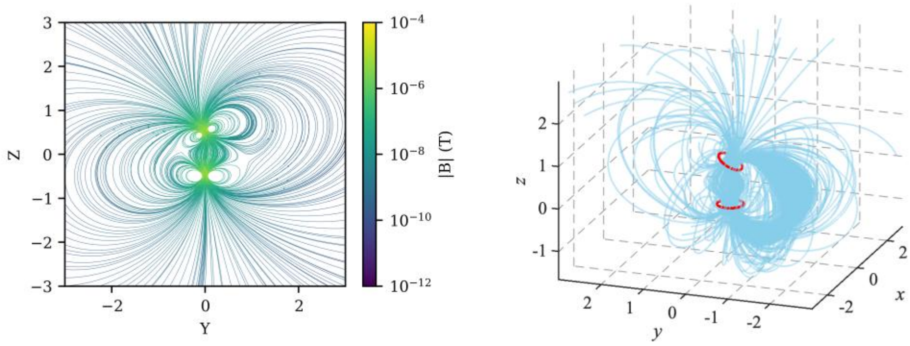

Figure 8. Magnetic topology of identical non-parallel coils with co-directional currents

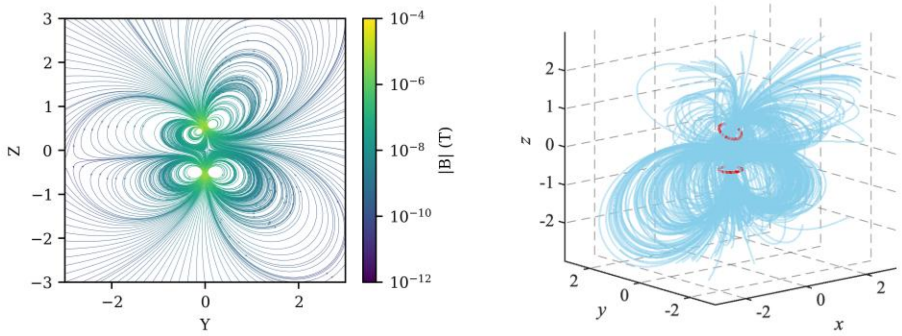

Figure 9. Magnetic topology of identical non-parallel coils with counter-directional currents

When two equal but non-parallel coils carry currents in the same direction or in opposite directions, the asymmetry becomes more pronounced. Under the same-direction current, the magnetic field forms a vortex-like structure in the intersection area of the two coils, with the streamlines spreading outward in a spiral pattern. The central area exhibits high field strength due to the superposition effect, while the edge area experiences a gradual decrease in the density of magnetic field lines due to the difference in angles; under the opposite-direction current, the magnetic field in the central area shows a tendency to cancel each other out, resulting in low field strength.

3.3. Magnetic Field of Multiple Circular Currents

Superposition of multiple circular currents underpins modeling of complex electromagnetic systems. The superposition principle enables decomposition of arbitrarily configured current ensembles into vector sums of individual loop contributions. This methodology proves essential for engineering applications including multipole magnets, electromagnetic arrays, and magnetic shielding devices.

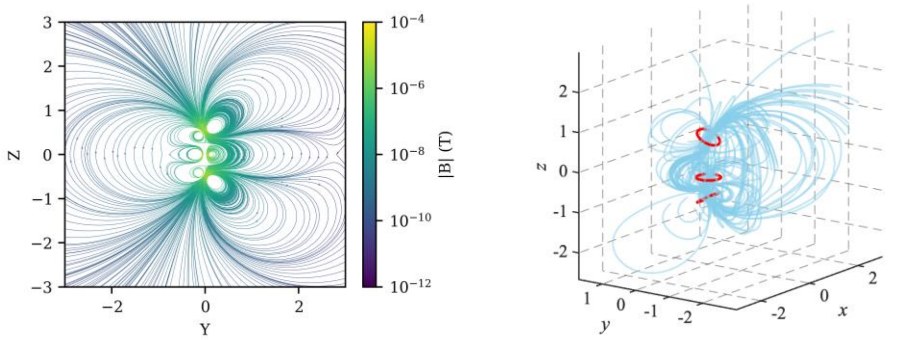

Figure 10. Magnetic topology of a three-coil configuration

For a three-coil system, constructive superposition generates a pronounced high-flux-density core at the centroid, surrounded by concentric toroidal isosurfaces manifesting radial field decay gradients. Asymmetric angular displacement of coils induces helical field rotation, producing complex vortex-like streamline patterns in 3D space. This coexistence of a core enhancement zone (from co-directional superposition) and peripheral cancellation regions (due to angular misalignment).

All the above-mentioned visualization results not only vividly present the superimposed effect of the magnetic fields under the configurations of parallel and reverse currents, verifying the applicability of the magnetic superposition principle under complex geometric conditions, but also systematically reveal the key characteristics of the magnetic field distribution, such as symmetrical distribution, continuous changes in intensity gradient, and the formation mechanism of local cancellation points. These characteristics not only deepen the understanding of the magnetic interaction mechanism of parallel circular currents, but also provide a visual basis for the parameterization design of electromagnetic devices. It is worth noting that the geometric parameters of the coil (such as angle offset, current direction) have a decisive regulatory effect on the spatial distribution of the magnetic field: by adjusting the arrangement of the coils, the distribution form of magnetic field intensity and the energy concentration area can be effectively controlled.

4. Conclusions and Future Work

This research is based on the Biot-Savart law, combined with numerical integration and the principle of field superposition. It has constructed magnetic field models for a single, two, and multiple ring currents, and achieved the visualization analysis of the magnetic field distribution through the collaborative simulation tools of Python and MATLAB. Visualization can deepen students' understanding of textbook knowledge. Through reproducible calculation models and visualization results, abstract electromagnetic concepts (such as magnetic field direction and intensity distribution) are transformed into graphics, providing an intuitive teaching tool for classroom teaching.

References

1. Wang Dalun. Comparative Study on the Calculation of Magnetic Field of Circular Current. *Journal of Southwest China Normal University (Natural Science Edition)* **2009**, 34 (01), 50-57. in Chinese
2. Li Yongping; Zhang Fan. The Magnetic Field Distribution of Circular Currents. *Journal of Jinan University* **1998**, (04), 61-64. in Chinese
3. Xu Shengnan; Ren Xuezhi; Wei Haojie; Zhan Kaiyun; Chen Wenjuan. Dynamic Simulation of Magnetic Field Distribution of Current-Carrying Ring Based on MATLAB. *College Physics Experiment* **2016**, 29 (03), 96-102. in Chinese
4. Wu Jinlong. Design of "Electromagnetic Field and Electromagnetic Waves" Virtual Simulation Experiments Based on MATLAB. *Modern Information Technology* **2024**, 8 (14), 194-198. in Chinese
5. Chen Wenqiong; Mei Zhonglei. Exploration of Electromagnetic Field Visualization Methods Based on Matlab. *Journal of Electrical and Electronic Teaching* **2022**, 44 (01), 140-143. in Chinese
6. Song Bixiong; Hu Haiyun. Application of Python in College Physics. *Physics and Engineering* **2019**, 29 (S1), 64-68. in Chinese
7. Xie Wenfa; Zhang Lutian; Liu Shihao. Application of Python Visualization Technology in Electrodynamics Teaching. *Physics and Engineering* **2024**, 34 (01), 92-96. in Chinese
8. Zhou Qunyi; Mo Yunfei; Zhou Lili; Hou Zhaoyang. MATLAB Visualization Method for Electric Field. *Physical Review* **2022**, (02), 18-24. in Chinese